Scaling laws for dual radio-frequency capacitively coupled discharges

T. H. Chung
Department of Physics, Dong-A University, Busan 604-714, Korea

(Received 9 August 2005; accepted 16 September 2005; published online 19 October 2005)

The characteristics of dual radio-frequency capacitively coupled discharges are studied based on a homogeneous analytic model. We are considering a planar plasma device that can be approximated using a one-dimensional model. A set of equations describing the dynamics of the system are presented and used to give the analytic scaling laws. Scaling laws relating the drive frequencies and the applied voltages of dual radio-frequency sources to operating functions such as plasma density and plasma potential are examined and compared with numerical simulations. © *2005 American Institute of Physics*. [DOI: 10.1063/1.2121327]

Capacitively coupled radio-frequency (CCRF) discharges are one of the most common plasma sources for thin-film deposition, etching, and plasma cleaning. In conventional CCRF, ion flux and ion energy, which play an important role in plasma processing, cannot be controlled separately. Independent control of ion flux and ion bombardment energy is possible in the dual frequency capacitively coupled plasma (DF CCP) sources.[1–3] This enables one to combine the high currents found at high frequency with high bias voltages. In DF CCP, the high-frequency power source controls plasma density and, hence, ion flux to the electrode while the low-frequency source controls ion acceleration toward the substrate. The sheath width, plasma potential, and ion energy can be controlled by the low-frequency source. Such a dual radio-frequency capacitively coupled plasma (CCP) has regained much interest in application to the etching of dielectric thin films.

In previous studies,[1–3] the increase of low-frequency voltage has been known to lead to the decrease in plasma density with a subsequent increase of sheath width until the discharge collapses. The increase in the sheath width is a direct result of the application of the low-frequency voltage, resulting in an increased total voltage. As the voltage of low-frequency power source increases, the sheath width of both electrodes increases. Then the capacitance gets smaller and the impedance of a discharge increases. For the fixed voltage of a high-frequency power source, the increase of the impedance results in the decrease of the conduction currents. In addition to this effect, with the increase in the voltage of the low-frequency source, the contribution of ohmic heating is reduced due to the decrease of the bulk region. From the particle balance equation based on a spatially averaged model,[4] the electron temperature is determined by the parameter pd (p is pressure and d is the effective plasma length). The increase of the sheath width causes the parameter pd to decrease and the electron temperature to increase.[3] As the ionization rate is dependent on the electron temperature, the plasma density decreases.

However, there have been many experiments and simulations that showed results contrary to this.[5,6] In this paper, we investigate the effect of the voltage of a low-frequency power source on the plasma density in DF CCP.

The discharge is driven with the sum of two sinusoidal rf currents oscillating at two different frequencies, ω_l and ω_h,

$$J_{\mathrm{rf}}(t) = J_l \cos(\omega_l t) + J_h \cos(\omega_h t), \tag{1}$$

where the subscripts l and h represent the low- and high-frequency sources, respectively. When the driven current is assumed to flow through the sheath entirely as the displacement current, we obtain the position of the plasma-sheath boundary,[7]

$$s(t) = \bar{s} - s_l \sin(\omega_l t) - s_h \sin(\omega_h t), \tag{2}$$

with

$$s_{l,h} = \frac{J_{l,h}}{en\omega_{l,h}}, \tag{3}$$

where $\bar{s}$ is the time-averaged sheath length and n is the density of immobile ions that can be assumed to be constant.

The voltage between two electrodes can be represented as the sum of two sinusoidal functions:

$$V(t) = V_l \sin(\omega_l t) + V_h \sin(\omega_h t), \tag{4}$$

with the amplitudes of

$$V_{l,h} = \frac{2en}{\epsilon_0}\bar{s}s_{l,h}, \tag{5}$$

where ϵ_0 is the permittivity of a vacuum.

The time-averaged voltage of Eq. (4) can be expressed as[7]

$$\bar{V} = \frac{3}{8} y V_l, \tag{6}$$

where y is written as

$$y = 1 + \frac{V_h}{V_l} - \frac{2}{3}\frac{V_h}{V_l + V_h}. \tag{7}$$

The power is transferred to the charged particles in the discharge by rf fields in the sheaths and bulk plasma. A mechanism in which the power is gained by the sheath is stochastic heating, ($\bar{S}_{\mathrm{stoc}}$) by the oscillating sheath plasma boundaries. A mechanism in which the power is gained by

bulk electrons is ohmic heating ($\bar{S}_{\mathrm{ohm}}$). Thus, the power gained by an electron is a sum of these, $\bar{S}_{\mathrm{el}}=\bar{S}_{\mathrm{stoc}}+\bar{S}_{\mathrm{ohm}}$.

Ohmic heating power can be written in terms of current density and resistance per unit area, R_{ohm},

$$\bar{S}_{\mathrm{ohm}}=\frac{1}{2}R_{\mathrm{ohm}}(J_l^2+J_h^2), \quad R_{\mathrm{ohm}}=\frac{m\nu_m d}{e^2 n}, \tag{8}$$

where m is the electron mass, e is the electronic charge, and ν_m is the electron collision frequency with neutrals.

From Eqs. (3) and (5), we can write

$$J_l^2+J_h^2=e^2n^2\left[\omega_l^2\left(\frac{\epsilon_0 V_l}{2en\bar{s}}\right)^2+\omega_h^2\left(\frac{\epsilon_0 V_h}{2en\bar{s}}\right)^2\right]. \tag{9}$$

The sheath width is related to the average sheath potential through the Child-Langmuir law,

$$en_s u_{\mathrm{B}} \propto \frac{\epsilon_0\left(\frac{2e}{M}\right)^{1/2}\bar{V}^{3/2}}{\bar{s}^2}, \tag{10}$$

where n_s is the plasma density at the sheath edge, u_{B} is the Bohm velocity, and M is the ion mass.

Extending the scaling formula for a single-frequency CCP (Refs. 4 and 8) to the DF CCP, we have

$$\bar{S}_{\mathrm{stoc}}\approx\left(\frac{m}{e}\right)^2\epsilon_0 T_e^{1/2}(\omega_l^2 V_l+\omega_h^2 V_h), \tag{11}$$

$$\bar{S}_{\mathrm{ohm}}\approx 1.73\frac{m}{2e}\epsilon_0\nu_m d T_e^{1/2}\frac{(\omega_l^2 V_l^2+\omega_h^2 V_h^2)}{\bar{V}^{3/2}}, \tag{12}$$

where T_e is the electron temperature and $\bar{S}_{\mathrm{stoc}}$ represents the heating power by the sheath of the driven electrode.

Since the stochastic heating is dominant for the most of the operating region, one can define the effective frequency and effective voltage,

$$\omega_{\mathrm{eff}}^2 V_{\mathrm{eff}}=\omega_l^2 V_l+\omega_h^2 V_h, \tag{13}$$

where

$$\omega_{\mathrm{eff}}^2=\frac{\omega_h^2+\left(\frac{V_l}{V_h}\right)^2\omega_l^2}{\left(\frac{V_l}{V_h}\right)^2+\frac{4}{3}\left(\frac{V_l}{V_h}\right)+1}. \tag{14}$$

Figure 1 shows the variation of $\bar{S}_{\mathrm{ohm}}$ and $\bar{S}_{\mathrm{stoc}}$ as a function of V_l/V_h for frequency ratios of 2/27 and 10/27 MHz. Here ν_m, d, T_e remain constant. The calculated values of $\bar{S}_{\mathrm{ohm}}$ are shown in units of $V_h^{1/2}$ per unit area, and $\bar{S}_{\mathrm{stoc}}$ in units of V_h per unit area. As can be seen, $\bar{S}_{\mathrm{ohm}}$ decreases with increasing low-frequency voltage for the fixed high-frequency voltage, and the slope becomes steep for the 2/27 MHz case. This is due to the fact that the 2/27 MHz case has a larger increase in $\bar{V}$ with V_l/V_h than that of the 10/27 MHz case. As can be seen, $\bar{S}_{\mathrm{stoc}}$ increases with increasing low-frequency voltage for the fixed high-frequency voltage, and the slope of variation becomes steeper for the 10/27 MHz case.

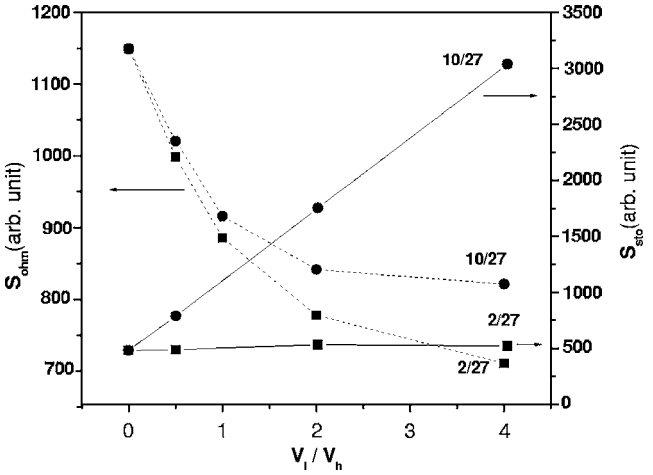

FIG. 1. The variations of $\bar{S}_{\mathrm{ohm}}$ in units of $V_h^{1/2}$ per unit area and $\bar{S}_{\mathrm{stoc}}$ in units of V_h per unit area as a function of V_l/V_h for frequency ratios of 2/27 and 10/27 MHz. Here ν_m, d, and T_e remain constant.

The sum of $\bar{S}_{\mathrm{ohm}}$ and $\bar{S}_{\mathrm{stoc}}, \bar{S}_{\mathrm{el}}$ for a fixed high-frequency voltage, has a shallow minimum at $V_l/V_h=1/2$, and increases with increasing low-frequency voltage for the 10/27 MHz case. However, for the 2/27 MHz case, $\bar{S}_{\mathrm{el}}$ decreases slightly with increasing low-frequency voltage. The figure of $\bar{S}_{\mathrm{el}}$ is skipped because it has a similar profile to that of the plasma density, which will be calculated in a next step.

$\bar{S}_{\mathrm{el}}$ must be equal to the power lost by collisions to the neutrals and that by escape from the plasma to the electrode. The total power absorbed by the plasma ($\bar{S}_{\mathrm{abs}}$) is equal to the power lost due to electron collision and due to escaping electrons and ions,

$$\bar{S}_{\mathrm{abs}}=2en_s u_B(\varepsilon_i+\varepsilon_c+2T_e), \tag{15}$$

where ε_c is the electron energy loss per ionization event, and ε_i is the ion kinetic energy that is almost equal to the average sheath potential, $\bar{V}$.

We can decompose $\bar{S}_{\mathrm{abs}}$ into $\bar{S}_{\mathrm{el}}$ and $\bar{S}_i$ (the power lost by ions),

$$\bar{S}_{\mathrm{el}}=2en_s u_B(\varepsilon_c+2T_e), \quad \bar{S}_i=2en_s u_B\bar{V}. \tag{16}$$

Then, we have

$$\bar{S}_{\mathrm{abs}}=\bar{S}_{\mathrm{el}}+\bar{S}_{\mathrm{el}}\frac{\bar{V}}{\varepsilon_c+2T_e}. \tag{17}$$

Rewriting this with $\bar{S}_{\mathrm{el}}=\bar{S}_{\mathrm{stoc}}+\bar{S}_{\mathrm{ohm}}$,

$$\bar{S}_{\mathrm{abs}}=\bar{S}_{\mathrm{ohm}}\left(1+\frac{\bar{V}}{\varepsilon_c+2T_e}\right)+\bar{S}_{\mathrm{stoc}}\left(1+\frac{\bar{V}}{\varepsilon_c+2T_e}\right). \tag{18}$$

In order to better understand the scaling behavior of plasma parameters of DF CCP, a simple model based on the energy balance can be used. The plasma density is determined by equating the power absorbed by electrons to the power lost by electrons and ions.

Therefore, equating Eq. (15) with Eq. (18), we have

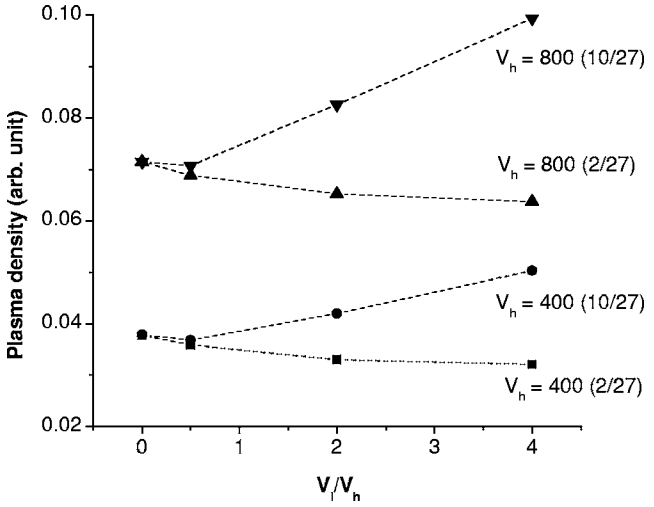

FIG. 2. The variation of plasma density as a function of V_l/V_h for frequency ratios of 2/27 and 10/27 MHz. Here $\nu_m=1.0\times10^7$ s^{-1}, $d=1.5$ cm, and $T_e=1.3$ eV are used.

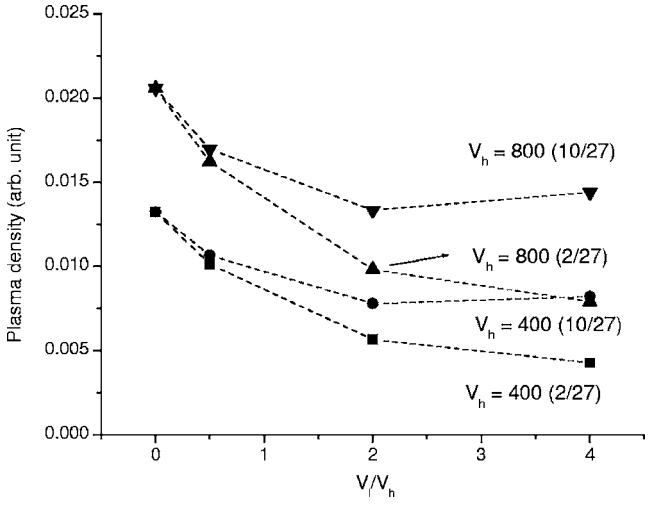

FIG. 3. The variation of plasma density as a function of V_l/V_h for frequency ratios of 2/27 and 10/27 MHz in higher-pressure discharges. Here $\nu_m=1.5\times10^8$ s^{-1}, $d=1.5$ cm, and $T_e=1.3$ eV are used.

$$n_s=\frac{1}{2eu_B}\frac{(\bar{S}_{\text{stoc}}+\bar{S}_{\text{ohm}})\left(1+\dfrac{\bar{V}}{\varepsilon_c+2T_e}\right)}{(\bar{V}+\varepsilon_c+2T_e)}. \tag{19}$$

The variation of the plasma density is calculated based on Eq. (19), considering Ar plasma with $\varepsilon_c=90$ eV, $T_e=1.3$ eV, $\nu_m=1.0\times10^7$ s^{-1}, $d=1.5$ cm. Figure 2 shows the variation of plasma density as a function of V_l/V_h for frequency ratios of 2/27 and 10/27 MHz and high-frequency voltages of 400 and 800 V. For the 10/27 MHz case, the plasma density has a shallow minimum at $V_l/V_h=1/2$, and increases with increasing low-frequency voltage, however, for the 2/27 MHz case, the plasma density decreases slightly with increasing low-frequency voltage. For single-frequency CCP, the plasma density is proportional to the rf voltage and the square of frequency.[8] In DF CCP, if the low-frequency voltage increases, the effective voltage increases but the effective frequency decreases.[7] The nonmonotonic behavior of plasma density is due to the competition of the effective voltage and the effective frequency.[6] For the 10/27 MHz case, the decrease of the effective frequency with increasing low-frequency voltage is not severe compared to that of the 2/27 MHz case. That is why the plasma density has a shallow minimum and increases again with increasing low-frequency voltage for the 10/27 MHz case. It should be noted that if we increase the frequency of the high-frequency source, for example, from 27 MHz to 60 or 100 MHz with the low-frequency 2 MHz fixed, the decrease of the effective frequency with increasing low-frequency voltage is not as severe as that of the 2/27 MHz case. Therefore, the plasma density does not decrease noticeably with increasing low-frequency voltage for the 2/60 and 2/100 MHz cases. This was observed in the particle-in-cell simulation study of DF CCP by Georgieva and Bogarts.[9]

For higher-pressure discharges, ($\nu_m=1.5\times10^8$ s^{-1}), in which ohmic heating is the dominant mechanism of power transfer, the trend changes. As shown in Fig. 3, for the 10/27 MHz case, the plasma density has a shallow minimum at $V_l/V_h=2$, and increases very slightly with increasing low-frequency voltage. However, for the 2/27 MHz case, the plasma density decreases with increasing low-frequency voltage. In the ohmic heating-dominated region, the plasma density is approximately proportional to the square root of rf voltage and the square of frequency. In this region, the effective voltage has a less profound effect on the plasma density. The scaling relations shown in Figs. 2 and 3 are in a reasonable agreement with particle-in-cell simulations[6,10] of asymmetric discharges.

It should be noted from Eq. (19) that the time-averaged sheath voltage $\bar{V}$ influences the scaling behavior of the plasma density. The time-averaged sheath voltage differs depending on the geometry of dual-frequency capacitive discharges, for example, depending on whether the discharge is symmetric or asymmetric, and whether two power sources are applied to one electrode or to different electrodes. That accounts for the different scaling behavior observed in various DF CCP systems.

At low pressures the ohmic heating is small compared to the stochastic heating. However, note that the contribution of ohmic heating is not negligible for most of the parameter region of interest in DF CCP. Most of the ohmic heating occurs at the plasma edge. Throughout the analysis in this study, we assume no variation of the electron temperature with low-frequency voltage. However, as the low-frequency voltage increases for the fixed high-frequency voltage, the electron energy distribution function and the effective electron temperature have been known to have a drastic change.[11] Therefore, the assumption of constant ν_m, d, T_e is very rough and needs further consideration.

In conclusion, a simple scaling formula based on the energy balance for predicting the behavior of the plasma density is derived and is compared with simulation results, finding good agreement. Especially, the effect of the voltage of the low-frequency power source on the plasma density is discussed in terms of the scaling formula.

ACKNOWLEDGMENT

This work is supported by the Research Fund of Dong-A University (the program year of 2004).

[1] P. C. Boyle, A. R. Ellingboe, and M. M. Turner, Plasma Sources Sci. Technol. **13**, 493 (2004).
[2] J. Robiche, P. C. Boyle, M. M. Turner, and A. R. Ellingboe, J. Phys. D **36**, 1810 (2003).
[3] P. C. Boyle, A. R. Ellingboe, and M. M. Turner, J. Phys. D **37**, 697 (2004).
[4] M. A. Lieberman and A. J. Lichtenberg, *Principles of Plasma Discharges and Material Processing* (Wiley, New York, 1994).
[5] T. Kitajima, Y. Takeo, Z. Lj. Petrovic, and T. Makabe, Appl. Phys. Lett. **77**, 489 (2000).
[6] H. C. Kim and J. K. Lee, J. Vac. Sci. Technol. A **A23**, 651 (2005).
[7] H. C. Kim, J. K. Lee, and J. W. Shon, Phys. Plasmas **10**, 4545 (2003).
[8] T. H. Chung, H. S. Yoon, and J. K. Lee, J. Appl. Phys. **78**, 6441 (1995).
[9] V. Georgieva and A. Bogaerts, J. Appl. Phys. **98**, 023308 (2005).
[10] J. K. Lee, N. Y. Babaeva, H. C. Kim, O. V. Manuilenko, and J. W. Shon, IEEE Trans. Plasma Sci. **32**, 47 (2004).
[11] H. C. Kim and J. K. Lee, Phys. Plasmas **12**, 053501 (2005).